

# Experimental transmission of quantum information using a superposition of causal orders

Yu Guo,<sup>1,2</sup> Xiao-Min Hu,<sup>1,2</sup> Zhi-Bo Hou,<sup>1,2</sup> Huan Cao,<sup>1,2</sup> Jin-Ming Cui,<sup>1,2</sup> Bi-Heng Liu,<sup>1,2,\*</sup>  
Yun-Feng Huang,<sup>1,2</sup> Chuan-Feng Li,<sup>1,2,†</sup> Guang-Can Guo,<sup>1,2</sup> and Giulio Chiribella<sup>3,4,‡</sup>

<sup>1</sup>CAS Key Laboratory of Quantum Information, University of Science and Technology of China, Hefei, 230026, People's Republic of China

<sup>2</sup>CAS Center For Excellence in Quantum Information and Quantum Physics,  
University of Science and Technology of China, Hefei 230026, P.R. China

<sup>3</sup>Department of Computer Science, The University of Hong Kong, Pokfulam Road, Hong Kong, P.R. China

<sup>4</sup>Department of Computer Science, University of Oxford, Parks Road, Oxford, UK

(Dated: January 22, 2020)

Communication in a network generally takes place through a sequence of intermediate nodes connected by communication channels. In the standard theory of communication, it is assumed that the communication network is embedded in a classical spacetime, where the relative order of different nodes is well-defined. In principle, a quantum theory of spacetime could allow the order of the intermediate points between sender and receiver to be in a coherent superposition. Here we experimentally realise a table-top simulation of this exotic possibility on a photonic system, demonstrating high-fidelity transmission of quantum information over two noisy channels arranged in a superposition of two alternative causal orders.

*Introduction.*— Communication from a sender to a receiver generally takes place through a series of intermediate nodes. For example, an email sent over the internet is generally relayed by a sequence of servers before landing in the receiver's inbox. Classically, the order of the intermediate nodes is always well-defined. The communication network is embedded in a classical spacetime where the causal relations between points are fixed. In quantum theory, instead, the superposition principle suggests that there may exist scenarios where spacetime itself is in a superposition of alternative configurations [1, 2]. A communication network embedded in a quantum spacetime could give rise to new scenarios where the communication channels act in a quantum superposition of orders [3, 4] or in some other form of indefinite order [5].

The extension of communication theory to scenarios where quantum channels act in a superposition of orders was recently addressed in a series of theoretical works [6–10]. These works demonstrated various advantages over the standard communication model of quantum Shannon theory [11], where the order of communication channels is well-defined. For example, Ref. [6] showed that two completely depolarising channels acting in a superposition of two orders can transmit a non-zero amount of classical information, whereas in the standard model they would completely block any kind of information. Similar advantages arise in the transmission of quantum information [7], sometimes leading to a complete removal of the noise [8]. To what extent these advantages are specific to superpositions of causal orders, rather than being generic to other forms of coherent superpositions of communication protocols, is currently a matter of debate [7, 9, 12–15]. Nevertheless, the advantages of the superposition of orders suggest that having access to quantum superpositions of spacetimes could have major consequences on the power of quantum communication networks.

The search for experimental evidence of quantum spacetimes has attracted increasing interest in recent years [16–19]. Still, no direct observation has been possible so far. An alternative approach is to simulate the superposition of space-

times through the already accessible physics taking place in a fixed, classical spacetime. The action of two communication channels connected in a quantum superposition of causal orders can be reproduced by setting up a mechanism that routes photons through two optical devices and controls the order in which the devices are visited [20–22]. In this way, it is possible to simulate quantum communication networks where the communication channels are embedded in a superposition of spacetimes, and to witness the advantages of the corresponding communication model.

Here we experimentally demonstrate the possibility of high-fidelity transmission of both classical and quantum information through noisy channels in a superposition of causal orders [6–8]. Our results offer a glance at exotic communication scenarios that could arise in quantum spacetimes, and, at the same time, contribute to the development of a new technology of coherent control over multiple transmission lines, with applications beyond the study of communication protocols with superpositions of orders. Indeed, the ability to coherently route photons through multiple optical devices enables not only communication in a superposition of causal orders, but also a variety of new communication protocols involving superpositions of alternative communication channels [9, 12, 23], superpositions of alternative directions of communication [24], and superpositions of alternative encoding/decoding operations [13]. The high level of accuracy achieved by our setup can also benefit the realization of these protocols, thereby contributing to the exploration of a broader class of quantum communication networks where the communication takes place in superpositions of alternative configurations.

*Background.*— In a standard communication scenario, a sender transmits messages to a receiver by encoding them in the internal state of a quantum particle and then sending it to the receiver through a sequence of noisy channels. The action of a generic quantum channel  $\mathcal{E}$  on a given quantum input state  $\rho$  is conveniently expressed in the Kraus representation  $\mathcal{E}(\rho) = \sum_i E_i \rho E_i^\dagger$ , where  $\{E_i\}$  are linear operators satisfy-

ing  $\sum_i E_i E_i^\dagger = I$ ,  $I$  being the identity operator.

The ability of a channel to transmit classical and quantum information is quantified by its classical capacity  $C$  and quantum capacity  $Q$ , respectively. The classical capacity  $C$  is the maximum number of bits that can be reliably transmitted per channel use, in the limit of asymptotically many channel uses [25, 26]. A lower bound on the classical capacity is provided by the one-shot accessible information

$$C_1 = \max_{\{p_x, \rho_x\}} \max_{\{P_y\}} H(X : Y) \quad (1)$$

where the maximum is over all possible input ensembles  $\{p_x, \rho_x\}$  and output measurements  $\{P_y\}$ , and  $H(X : Y)$  is the mutual information between  $x$  and  $y$ .

The quantum capacity  $Q$  is the maximum number of qubits that can be reliably transmitted per channel use, again in the limit of asymptotically many uses [27–29]. A lower bound to the quantum capacity is the one-shot coherent information

$$Q_1 = \max_{\rho} \mathcal{I}_c(\rho) \quad (2)$$

where  $\mathcal{I}_c(\rho) := S[\mathcal{E}(\rho)] - S_e(\rho, \mathcal{E})$  is the coherent information of the state  $\rho$  [30], defined in terms of the von Neumann entropy  $S(\rho) := -\text{Tr}[\rho \log_2 \rho]$ , and of the entropy exchange  $S_e(\rho, \mathcal{E}) := S[(\mathcal{I}_R \otimes \mathcal{E})(|\Psi_\rho\rangle\langle\Psi_\rho|)]$ ,  $|\Psi_\rho\rangle$  being any purification of  $\rho$  using a reference quantum system  $R$ .

*Communication networks and superposition of orders.*—

In a network scenario, the communication between a sender and a receiver proceeds through a sequence of intermediate nodes, located at different spacetime points and connected by communication channels. Here we consider the case of  $n = 2$  channels,  $\mathcal{E}$  and  $\mathcal{F}$ , the former connecting spacetime points  $P$  and  $P'$ , and the latter connecting spacetime points  $Q$  and  $Q'$ .

In the standard setting, the causal relations among spacetime points are well-defined, and so is the order of the intermediate nodes between the sender and receiver, located at spacetime points  $S$  and  $R$ , respectively. For example, one can have the order  $S \preceq P \preceq P' \preceq Q \preceq Q' \preceq R$ , indicating that signals can be transmitted from  $S$  to  $P$ , from  $P$  to  $P'$ , and then to  $Q$  and to  $Q'$ . Assuming that no noise takes place in the transmission from  $S$  to  $P$ ,  $P'$  to  $Q$ , and  $Q$  to  $R$ , this configuration leads to the overall channel  $\mathcal{F}\mathcal{E}$  connecting the sender and receiver. In another spacetime configuration, one could have the order  $S \preceq Q \preceq Q' \preceq P \preceq P' \preceq R$ , corresponding to the channel  $\mathcal{E}\mathcal{F}$ . In either configurations, the sender and receiver are assumed to know the structure of spacetime, and therefore to know whether the overall channel between them is  $\mathcal{E}\mathcal{F}$  or  $\mathcal{F}\mathcal{E}$ .

New possibilities arise when the background spacetime is treated quantum mechanically [7]. One can associate the basic configurations  $S \preceq P \preceq P' \preceq Q \preceq Q' \preceq R$  and  $S \preceq Q \preceq Q' \preceq P \preceq P' \preceq R$  to two orthogonal states  $|0\rangle$  and  $|1\rangle$ , forming a basis for an effective two-dimensional quantum system, called the *order qubit*. The order qubit can be interpreted as a coarse-grained description of a quantum spacetime in which the communication network is embedded. In

this scenario, the basis states  $|0\rangle$  and  $|1\rangle$  represent two distinct semi-classical states of the gravitational field. Coherent superpositions semi-classical states arise generically across various theories of quantum gravity [17–19].

The insertion of two quantum channels  $\mathcal{E}$  and  $\mathcal{F}$  into a quantum spacetime in the state  $\omega$  can be described by the quantum SWITCH (QS) transformation [3, 4]  $\mathcal{S}_\omega : (\mathcal{E}, \mathcal{F}) \mapsto \mathcal{S}_\omega(\mathcal{E}, \mathcal{F})$ , defined as

$$\mathcal{S}_\omega(\mathcal{E}, \mathcal{F})(\rho) := \sum_{i,j} W_{ij}(\rho \otimes \omega) W_{ij}^\dagger, \quad (3)$$

with

$$W_{ij} := E_i F_j \otimes |0\rangle\langle 0| + F_j E_i \otimes |1\rangle\langle 1|, \quad (4)$$

where  $\{E_i\}$  and  $\{F_j\}$  are the Kraus operators of  $\mathcal{E}$  and  $\mathcal{F}$ . The quantum channel (3) can be reproduced in the ordinary, classically-well defined spacetime, using *e.g.* photonic systems [20–22].

It is worth noting that quantum channel (3) is independent of the choice of Kraus operators  $\{E_i\}$  and  $\{F_j\}$ . Physically, this means that, in principle, its realization does not require access to the environment of the communication devices. This is not the case, however, in all the existing implementations of the channel  $\mathcal{S}_\omega(\mathcal{E}, \mathcal{F})$  (including the present one), where access to the environments of both channels  $\mathcal{E}$  and  $\mathcal{F}$  is essential for producing the superposition of causal orders while operating in a classical spacetime [9, 31].

The interference between the two alternative orders provides advantages over standard quantum Shannon theory, enabling communication through channels that individually block information [6–9]. While these advantages crucially rely on the order qubit being used to assist the decoding, it is worth stressing that they do not use the order qubit as a way to bypass the given communication channels. Indeed, the transformation of resources  $\mathcal{S}_\omega : (\mathcal{E}, \mathcal{F}) \mapsto \mathcal{S}_\omega(\mathcal{E}, \mathcal{F})$  does not give the sender and the receiver a way to transmit information independently of the channels  $\mathcal{E}$  and  $\mathcal{F}$  [7, 15].

The advantages in Refs. [6–9] involve pairs of Pauli channels, of the form  $\mathcal{E}_{\vec{p}} = \sum_{i=0}^3 p_i \sigma_i \rho \sigma_i$  and  $\mathcal{F}_{\vec{q}} = \sum_{i=0}^3 q_i \sigma_i \rho \sigma_i$ , where  $(\sigma_0, \sigma_1, \sigma_2, \sigma_3)$  are the Pauli matrices  $(I, X, Y, Z)$ . Suppose that the two channels  $\mathcal{E}_{\vec{p}}$  and  $\mathcal{F}_{\vec{q}}$  are combined in a superposition of orders, with the control qubit in the state  $\omega = |+\rangle\langle +|$ . From Equations (3) and (4), the resulting channel  $\mathcal{S}_\omega(\mathcal{E}_{\vec{p}}, \mathcal{F}_{\vec{q}})$  acts as

$$\mathcal{S}(\mathcal{E}_{\vec{p}}, \mathcal{F}_{\vec{q}})(\rho) = r_+ \mathcal{C}_+(\rho) \otimes |+\rangle\langle +| + r_- \mathcal{C}_-(\rho) \otimes |-\rangle\langle -|, \quad (5)$$

where  $r_+$  and  $r_-$  are the probabilities defined by  $r_- := r_{12} + r_{23} + r_{13}$ ,  $r_{ij} := p_i q_j + p_j q_i$ , and  $r_+ := 1 - r_-$ , and  $\mathcal{C}_+$  and  $\mathcal{C}_-$  are the Pauli channels defined by

$$\mathcal{C}_+ = \frac{(\sum_{i=0}^3 r_{ii}/2)\rho + \sum_{i=1}^3 r_{0i} \sigma_i \rho \sigma_i}{r_+} \quad (6)$$

and

$$\mathcal{C}_- = \frac{[r_{12} \sigma_3 \rho \sigma_3 + r_{23} \sigma_1 \rho \sigma_1 + r_{31} \sigma_2 \rho \sigma_2]}{r_-}. \quad (7)$$

Hence, a receiver who measures the order qubit in the Fourier basis  $\{|+\rangle, |-\rangle\}$  can separate the two channels  $\mathcal{C}_+$  and  $\mathcal{C}_-$ , and adapt the decoding operations to them.

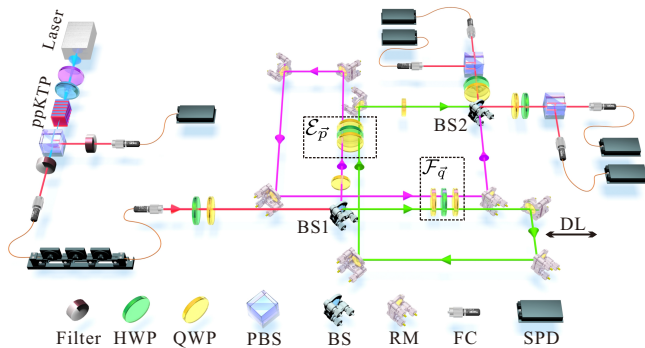


FIG. 1. Experimental setup. A cw violet laser (power is 2 mW, working at 404 nm) is incident on and pumps a type-II cut ppKTP crystal generating photon pairs of degenerate wavelength at 808 nm. One of the photons acts as a trigger and the other is used to transmit information from sender to receiver. In the QS, the information is encoded in photon's polarization states while its spatial modes act as the control qubit. The Pauli channels,  $\mathcal{E}_{\vec{p}}$  and  $\mathcal{F}_{\vec{q}}$ , are each composed of two QWPs and a HWP. A trombone-arm delay line and a PZT are used to set the path length and the relative phases of the interferometer. HWPs were used after BS1 and before BS2 to compensate the reflection phases introduced by the BSs. HWP: half wave plate; QWP: quarter wave plate; PBS: polarizing beam splitter; BS: beam splitter ( $T/R = 50/50$ ); RM: reflection mirror; FC: fiber coupler; SPD: single photon detector; DL: trombone-arm delay line.

*Experimental implementation.*— In our experiment, we demonstrated the three communication protocols of Refs. [6–8] to a high degree of accuracy. As shown in Fig. S1, photon pairs were generated by means of the process of spontaneous parametric down conversion. The idler photon was used as a herald and the target photon was fed into the quantum channel after encoding by the sender and then detected by the receiver. In our realisation of the switched channel (S4), photonic polarization acts as the information carrying qubit, while the spatial modes are used as the order qubit. Spatial modes were introduced by BS1 to switch the two channels  $\mathcal{E}_{\vec{p}}$  and  $\mathcal{F}_{\vec{q}}$ , and BS2 was used to project the control qubit onto  $|\pm\rangle_c$ . We assembled two quarter wave plates (QWP) and a half wave plate (HWP) to achieve the operations  $\sigma_0, \sigma_1, \sigma_2$ , and  $\sigma_3$ . After these four operations were applied in four separate experiments, arbitrary Pauli channel  $\mathcal{E}_{\vec{p}}$  can be obtained by post-processing the experimental outcomes, mixing its statistics with probabilities  $\vec{p}$ .

To fully characterize the action of the channel  $\mathcal{S}_\omega(\mathcal{E}, \mathcal{F})$  on an arbitrary input state  $\rho$ , we performed quantum process tomography [32–34], where the sender prepared signal states  $|H\rangle, |V\rangle, |D\rangle, |A\rangle, |R\rangle$ , and  $|L\rangle$  and the observables  $\sigma_1, \sigma_2$ ,

and  $\sigma_3$  were measured by the receiver. A generic channel  $\mathcal{E}$  can be reconstructed from the matrix  $\gamma_{ij}$  in the expression  $\mathcal{E}(\rho) = \sum_{ij} \gamma_{ij} \sigma_i \rho \sigma_j$ .

*Quantum communication with entanglement-breaking channels.*— Consider a bit flip channel  $\mathcal{B}_s(\rho) = (1-s)\rho + s\sigma_1\rho\sigma_1$  and a phase flip channel  $\mathcal{P}_t(\rho) = (1-t)\rho + t\sigma_3\rho\sigma_3$ , corresponding to Pauli channels  $\mathcal{E}_{\vec{p}}$  and  $\mathcal{F}_{\vec{q}}$  with  $\vec{p} = (1-s, s, 0, 0)$  and  $\vec{q} = (1-t, 0, 0, t)$ , respectively [7]. For  $s = t = 1/2$ , the two channels are entanglement-breaking, and therefore unable to transmit any quantum information. In contrast, the channel  $\mathcal{C}_-$  of Equation (7) is the unitary gate  $\sigma_2$ , and therefore it allows for the noiseless heralded transmission of a qubit, meaning that the receiver can decode the message without any error through the channel  $\mathcal{C}_-$ .

The possibility of noiseless heralded quantum communication is an important difference between the communication model with independent quantum channels in a superposition of orders and a related communication model with independent quantum channels traversed in a superposition of paths [9, 12, 23]. The transmission of quantum information through one of two channels  $\mathcal{E}$  and  $\mathcal{F}$  is described by a controlled-channel with Kraus operators [9, 12, 35]

$$W'_{ij} = \beta_j E_i \otimes |0\rangle\langle 0| + \alpha_i F_j \otimes |1\rangle\langle 1|, \quad (8)$$

where  $\alpha_i$  and  $\beta_j$  are complex amplitudes, and the states  $|0\rangle$  and  $|1\rangle$  represent paths of the information carrier, going through channels  $\mathcal{E}$  and  $\mathcal{F}$ , respectively. In this setting, Gisin *et al* showed that preparing the path in a coherent superposition leads to a heralded reduction of the noise [23]. More recently, it was shown that the superposition of paths can also increase the overall capacity, enabling deterministic communication through depolarizing channels [12] and even complete erasure channels [9].

The communication enhancements due to superpositions of paths (8) and superposition of orders (4) share several common features, in particular the crucial role of coherence between alternative configurations of the communication channels. Nevertheless, they also exhibit interesting differences. One such difference concerns the possibility of noiseless heralded communication: while placing two independent noisy channels in a superposition of orders can lead to heralded noiseless communication, placing them on two alternative paths only lead to a partial noise reduction [7, 8]. Interestingly, this feature is balanced by the fact that communication enhancements due to superpositions of paths are more common, while the enhancements due to the superposition of order require a specific matching between coherence in the superposition and commutativity of the channels [14].

While every real experiment involves noise and imperfections, the in-principle possibility of noiseless communication through superposition of orders suggests that the experimental fidelities can be arbitrarily close to 1. In our experiment, we pushed towards this target by adopting a phase-locked system (described in Ref. [36]) to ensure the stability of the path interferometer. Thanks to phase locking, we managed to obtain

an average fidelity of  $0.9747 \pm 0.0012$  with the unitary gate  $\sigma_2$  predicted by the theory. In addition, we used the reconstructed channel matrix  $\gamma_{ij}$  to find the input state that maximises the coherent information in Eq. (S3). The optimisation can be reduced to three real parameters  $(\alpha, \theta, \psi)$  by parameterising the qubit state  $\rho$  as  $\rho = \alpha_0|\phi\rangle\langle\phi| + (1-\alpha_0)|\phi_\perp\rangle\langle\phi_\perp|$ , where  $|\phi\rangle = \cos(\theta)|0\rangle + \sin(\theta)e^{i\psi}|1\rangle$  and  $|\phi_\perp\rangle = \sin(\theta)|0\rangle - \cos(\theta)e^{i\psi}|1\rangle$  are basis states. Since the entropy exchange is independent of the choice of purification, the parameters  $(\alpha_0, \theta, \psi)$  completely determine the coherent information.

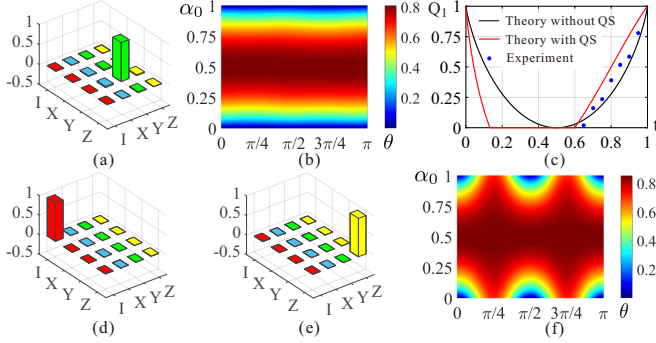


FIG. 2. Transmission of quantum information through entanglement-breaking channels in a superposition of causal orders. (a) Real part of the reconstructed matrix of  $\mathcal{S}(\mathcal{B}_s, \mathcal{P}_t)$ , for  $s = t = 1/2$ . (b) Coherent information  $\mathcal{I}_c$  for the channel  $\mathcal{C}_-$  with  $s = t = \frac{1}{2}$  as a function of  $\theta$  and  $\alpha_0$ , for fixed  $\psi = 0.790\pi$ . (c) One-shot coherent information  $Q_1$  for the channel  $\mathcal{S}(\mathcal{B}_t, \mathcal{P}_t)$  with  $t \in [0, 1]$ . The experimental results are marked as blue dots, while the correspond theoretical predictions are plotted in the red line. For comparison, the one-shot coherent information of the two dephasing channels combined in a definite order is also shown in the black line. (d-e) Real parts of the reconstructed matrices of  $\mathcal{C}_+$  and  $\mathcal{C}_-$  of the channel  $\mathcal{S}(\mathcal{F}, \mathcal{F})$ . (f) Coherent information  $\mathcal{I}_c$  for channel  $\mathcal{S}(\mathcal{F}, \mathcal{F})$  as a function of  $\theta$  and  $\alpha_0$ , for fixed  $\psi = 0.155\pi$ . Error bars are not visible in the figure as they are smaller than the marker size.

Fig. 2 shows the experimental results for the coherent information  $\mathcal{I}_c$  of the channel  $\mathcal{C}_-$  and of the whole channel  $\mathcal{S}(\mathcal{B}_s, \mathcal{P}_t)$ . For channel  $\mathcal{C}_-$ , the result is a one-shot coherent information  $Q_1$  of about  $0.812 \pm 0.003$ , obtained with parameters  $\alpha_0 = 0.500$ ,  $\theta = 0.0723\pi$ , and  $\psi = 0.790\pi$ . The dependence of the coherent information  $\mathcal{I}_c$  on  $\alpha_0$  and  $\theta$  is shown in Fig. 2 (b) for fixed  $\psi = 0.790\pi$ . More generally,  $Q_1$  of the channel  $\mathcal{S}(\mathcal{B}_s, \mathcal{P}_t)$  is further show in Fig. 2 (c) as a function of  $t$ , with  $s = t$ . One can find out that, as long as  $t > 0.62$ ,  $Q_1$  of  $\mathcal{S}(\mathcal{B}_t, \mathcal{P}_t)$  (red line) surpasses the coherent information when the two channels are combined in a fixed order (black line). Our results (blue dots) verified the existence of the advantage of indefinite causal order and the possibility of heralded, high-fidelity communication. The deviation of the channel capacities from their theoretical predictions are due to imperfect channel simulations and measurement error.

An even more radical example of transmission of quantum information in a superposition of order corresponds to two entanglement-breaking channels  $\mathcal{F}(\rho) = 1/2(\sigma_1\rho\sigma_1 + \sigma_2\rho\sigma_2)$  [8]. In normal conditions, the channel  $\mathcal{F}$  cannot trans-

mit any quantum information. Still, when two such channels are inserted in the QS, the channels  $\mathcal{C}_+$  and  $\mathcal{C}_-$  are both unitary, enabling the deterministic noiseless transmission of one qubit. This effect is more dramatic than the aforementioned heralded noiseless communication, as heralded noiseless transmission alone is not enough to guarantee a non-zero quantum capacity.

In our experiment, we find that the channels  $\mathcal{C}_+$  and  $\mathcal{C}_-$  have fidelities  $0.9823 \pm 0.0013$  and  $0.9846 \pm 0.0014$  with the corresponding unitary gates (Fig. 2 (d-e)). The one-shot coherent information  $Q_1$  is  $0.855 \pm 0.004$  and can be obtained when  $\alpha_0 = 0.500$ ,  $\theta = 0.7575\pi$ , and  $\psi = 0.155\pi$ . Fig. 2 (f) reports the result of coherent information  $\mathcal{I}_c$  of channel  $\mathcal{S}(\mathcal{F}, \mathcal{F})$  varying with the parameters  $\alpha_0$  and  $\theta$ , while  $\psi$  is set to be  $0.155\pi$ .

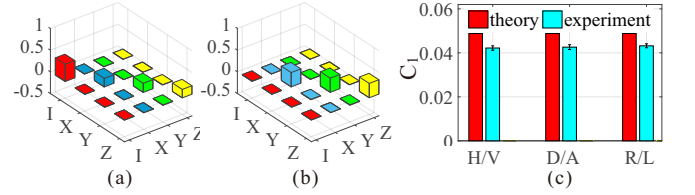


FIG. 3. Communication of classical information through depolarizing channels. (a-b) Real parts of the matrices of  $\mathcal{C}_+$  and  $\mathcal{C}_-$  for the channel  $\mathcal{S}(\mathcal{D}, \mathcal{D})$ . (c) Mutual information for  $\mathcal{S}(\mathcal{D}, \mathcal{D})$ , when encoding and decoding with H/V, D/A, and R/L. Results from theory and experiments are represented by red and green bars respectively.

*Transmitting classical information with depolarising channels.*— Consider two completely depolarising channels  $\mathcal{D}(\rho) = 1/4 \sum_{i=0}^3 \sigma_i \rho \sigma_i$ . In this case, the resulting channels  $\mathcal{C}_+$  and  $\mathcal{C}_-$  can transmit classical information, despite the fact that no classical information can be sent through each depolarising channel individually [6]. This scenario demonstrates an advantage over all communication protocols where multiple depolarising channels are used in a sequence, and any intermediate operation between them does not transfer information from the internal degrees of freedom of the particle to its path [9]. This protocol was experimentally demonstrated in Ref. [37] using orbital angular momentum modes as the information carriers. Our implementation uses polarisation states, which achieve a higher communication performance, allowing us to demonstrate a non-zero communication capacity with more than 38.7 standard deviations.

Fig. S2 (a-b) illustrate the real parts of  $\mathcal{C}_+$  and  $\mathcal{C}_-$  of reconstructed  $\mathcal{S}(\mathcal{D}, \mathcal{D})$  (see the imaginary parts in Ref. [36]). The fidelities are  $0.9989 \pm 0.0001$  and  $0.9903 \pm 0.0017$ , thereby establishing the high quality of our channel. To lower bound the classical capacity, we chose three kinds of signal states, specifically,  $\{|H\rangle, |V\rangle\}$ ,  $\{|D\rangle, |A\rangle\}$ , and  $\{|R\rangle, |L\rangle\}$ ; the input distribution  $p(x)$  is set to maximize the mutual information according to Eq. (S2). The mutual information with respect to these three choices of signal states is  $0.0422 \pm 0.0010$ ,  $0.0426 \pm 0.0011$ , and  $0.0432 \pm 0.0009$ , matching well the theoretical value of 0.0488 (Fig. S2(c)). The error bars are esti-

mated by Monte Carlo simulations.

*Conclusion.*— We have experimentally demonstrated the high-fidelity transmission of quantum information through communication channels in a coherent superposition of alternative orders. Our experiments can be viewed as simulations of exotic communication scenarios where the sender and the receiver are embedded in a quantum spacetime, and the order between the noisy processes occurring in two different regions is indefinite. At the same time, the accurate coherent control over multiple communication lines, achieved in our setup, is a flexible primitive that can also be used to demonstrate more general communication advantages, arising from superpositions of paths [9, 12, 23], directions of communication [24], or encoding operations [13]. Our results suggest that coherent control over multiple communication channels may also have applications to quantum communication in the ordinary, classically well-defined spacetime.

[*Note added.* During the preparation of this manuscript, the authors became aware of a work by K. Goswami et al [37], that independently demonstrated the enhanced effect of a superposition of causal orders on transmitting classical information.]

*Acknowledgments.*— We thank Kang-Da Wu, Jin-Shi Xu, Xiao-Ye Xu, Chao Zhang, Kai Sun and Yong-Xiang Zheng for valuable discussions. This work was supported by the National Key Research and Development Program of China (No. 2017YFA0304100, 2016YFA0301300, 2016YFA0301700), NSFC (Nos. 11774335, 11504253, 11874345, 11821404, 11675136), the Key Research Program of Frontier Sciences, CAS (No. QYZDY-SSW-SLH003), the Fundamental Research Funds for the Central Universities, the Anhui Initiative in Quantum Information Technologies (Nos. AHY020100, AHY060300), the John Templeton Foundation (grant 60609, Quantum Causal Structures), the Croucher Foundation, and the Hong Research Grant Council through grants 17326616 and 17307719. This publication was made possible through the support of a grant from the John Templeton Foundation. The opinions expressed in this publication are those of the authors and do not necessarily reflect the views of the John Templeton Foundation.

---

\* [bhliu@ustc.edu.cn](mailto:bhliu@ustc.edu.cn)

† [cffi@ustc.edu.cn](mailto:cffi@ustc.edu.cn)

‡ [giulio.chiribella@cs.ox.ac.uk](mailto:giulio.chiribella@cs.ox.ac.uk)

- [1] C. Rovelli, *Quantum Gravity* (Cambridge University Press, 2004).
- [2] L. Hardy, *Journal of Physics A: Mathematical and Theoretical* **40**, 3081 (2007).
- [3] G. Chiribella, G. M. D’Ariano, P. Perinotti, and B. Valiron, *Physical Review A* **88**, 022318 (2013).
- [4] G. Chiribella, *Physical Review A* **86**, 040301 (2012).
- [5] O. Oreshkov, F. Costa, and Č. Brukner, *Nature communications* **3**, 1092 (2012).
- [6] D. Ebler, S. Salek, and G. Chiribella, *Physical review letters* **120**, 120502 (2018).
- [7] S. Salek, D. Ebler, and G. Chiribella, arXiv preprint arXiv:1809.06655 (2018).
- [8] G. Chiribella, M. Banik, S. S. Bhattacharya, T. Guha, M. Alimuddin, A. Roy, S. Saha, S. Agrawal, and G. Kar, arXiv preprint arXiv:1810.10457 (2018).
- [9] G. Chiribella and H. Kristjánsson, *Proceedings of the Royal Society A* **475**, 20180903 (2019).
- [10] L. M. Procopio, F. Delgado, M. Enríquez, N. Belabas, and J. A. Levenson, *Entropy* **21**, 1012 (2019).
- [11] M. M. Wilde, *Quantum information theory* (Cambridge University Press, 2013), ch. 24.7.2.
- [12] A. A. Abbott, J. Wechs, D. Horsman, M. Mhalla, and C. Branciard, arXiv preprint arXiv:1810.09826 (2018).
- [13] P. A. Guérin, G. Rubino, and Č. Brukner, *Physical review A* **99**, 062317 (2019).
- [14] N. Loizeau and A. Grinbaum, arXiv preprint arXiv:1906.08505 (2019).
- [15] H. Kristjánsson, S. Salek, D. Ebler, and G. Chiribella, arXiv:1910.08197 (2019).
- [16] S. Hossenfelder, *Experimental search for quantum gravity* (Springer, 2017).
- [17] S. Bose, A. Mazumdar, G. W. Morley, H. Ulbricht, M. Toroš, M. Paternostro, A. A. Geraci, P. F. Barker, M. Kim, and G. Milburn, *Physical review letters* **119**, 240401 (2017).
- [18] C. Marletto and V. Vedral, *Physical review letters* **119**, 240402 (2017).
- [19] M. Christodoulou and C. Rovelli, *Physics Letters B* **792**, 64 (2019).
- [20] L. M. Procopio, A. Moqanaki, M. Araújo, F. Costa, I. A. Calafell, E. G. Dowd, D. R. Hamel, L. A. Rozema, Č. Brukner, and P. Walther, *Nature communications* **6**, 7913 (2015).
- [21] G. Rubino, L. A. Rozema, A. Feix, M. Araújo, J. M. Zeuner, L. M. Procopio, Č. Brukner, and P. Walther, *Science Advances* **3**, e1602589 (2017).
- [22] K. Goswami, C. Giarmatzi, M. Kewming, F. Costa, C. Branciard, J. Romero, and A. G. White, *Phys. Rev. Lett.* **121**, 090503 (2018).
- [23] N. Gisin, N. Linden, S. Massar, and S. Popescu, *Physical Review A* **72**, 012338 (2005).
- [24] F. Del Santo and B. Dakić, *Physical Review Letters* **120**, 060503 (2018).
- [25] A. S. Holevo, *IEEE Transactions on Information Theory* **44**, 269 (1998).
- [26] B. Schumacher and M. D. Westmoreland, *Physical Review A* **56**, 131 (1997).
- [27] S. Lloyd, *Physical Review A* **55**, 1613 (1997).
- [28] P. W. Shor, in *lecture notes, MSRI Workshop on Quantum Computation* (2002).
- [29] I. Devetak, *IEEE Transactions on Information Theory* **51**, 44 (2005).
- [30] B. Schumacher and M. A. Nielsen, *Physical Review A* **54**, 2629 (1996).
- [31] O. Oreshkov, arXiv preprint arXiv:1801.07594 (2018). *Quantum* **3**, 206 (2019).
- [32] I. L. Chuang and M. A. Nielsen, *Journal of Modern Optics* **44**, 2455 (1997).
- [33] G. D’Ariano and P. L. Presti, *Physical review letters* **86**, 4195 (2001).
- [34] M. F. Sacchi, *Physical Review A* **63**, 054104 (2001).
- [35] D. K. Oi, *Physical review letters* **91**, 067902 (2003).
- [36] See Supplemental Material for more details.
- [37] K. Goswami, J. Romero, and A. White, arXiv preprint arXiv:1807.07383 (2018).

## Supplementary Materials for Experimental transmission of quantum information using a superposition of causal orders

*Phase locking effect.*— We used a phase locked system composed by piezoelectric transducer to overcome the phase drift of the Mach-Zehnder (MZ) interferometer in the quantum switch caused by air turbulence. We observed, as shown in Fig. S1, the phase stability of the MZ interferometer for two hours, between which an extra relative phase of  $\pi$  was added between the two spatial modes at the point of one hour. The overall visibility during this time was 0.979. In our experiment, to switch two Pauli channels, we need to perform  $4 \times 4 = 16$  separate experiments to obtain all needed operations. To perform quantum process tomography of the switched channels, we need to prepare 6 kind of signal states, i.e.  $|H\rangle$ ,  $|V\rangle$ ,  $|D\rangle$ ,  $|A\rangle$ ,  $|R\rangle$ , and  $|L\rangle$  and reconstruct all the out put states, which requires 3 observables  $\sigma_1$ ,  $\sigma_2$ , and  $\sigma_3$  to be measured. So, the total number of measurement settings would be  $16 \times 6 \times 3 = 288$ . As each setting took 4 s to collect the data and 3 s to set the angles of the half wave plates and quarter wave plates, the total measurement time was under 35 min. The visibility of our setup during this time was maintained at high quality.

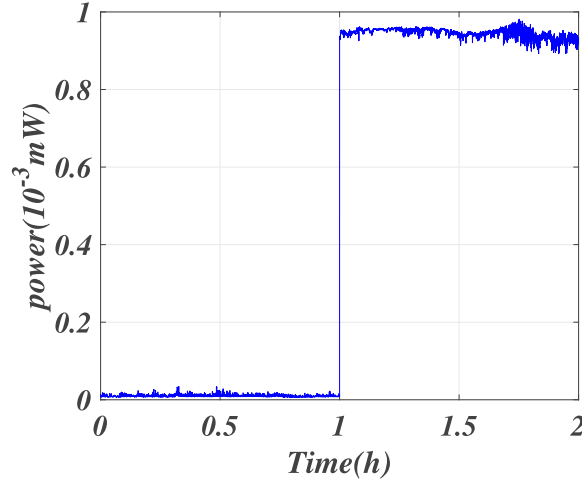


FIG. S1. Result of visibility of the MZ interferometer in two hours. At the point of 1 hour, an extra phase of  $\pi$  was added between spatial mode 1 and spatial mode 2. The overall visibility remained 0.979 during this period.

*Communication through switched Pauli channel.*— The Kraus representation of a generic Pauli channel is given by

$$\mathcal{E}_{\vec{p}} = \sum_{i=0}^3 p_i \sigma_i \rho \sigma_i, \quad (\text{S1})$$

where Pauli operators  $\sigma_i$  are in the set  $\{I, X, Y, Z\}$  and  $\vec{p} = (p_0, p_1, p_2, p_3)$  denotes  $\sigma_i$ 's probability vector. When two Pauli channels with probability vectors of  $\vec{p} = (p_0, p_1, p_2, p_3)$  and  $\vec{q} = (q_0, q_1, q_2, q_3)$  assembled in a quantum switch, the new channel, noted as  $\mathcal{S}(\mathcal{E}_{\vec{p}}, \mathcal{E}_{\vec{q}})(\rho)$  here, can be defined as

$$\mathcal{S}(\mathcal{E}_{\vec{p}}, \mathcal{E}_{\vec{q}})(\rho) = \sum_{i,j=0}^3 W_{ij}(\rho \otimes |c\rangle\langle c|) W_{ij}^\dagger, \quad (\text{S2})$$

with its Kraus operators

$$W_{ij} = \sqrt{p_i q_j} \sigma_i \sigma_j \otimes |0\rangle\langle 0|_c + \sqrt{q_j p_i} \sigma_j \sigma_i \otimes |1\rangle\langle 1|_c. \quad (\text{S3})$$

From Eq. S1 and Eq. S2, the output state of the channel

$$\mathcal{S}(\mathcal{E}_{\vec{p}}, \mathcal{E}_{\vec{q}})(\rho) = r_+ \mathcal{C}_+(\rho) \otimes |+\rangle\langle +| + r_- \mathcal{C}_-(\rho) \otimes |-\rangle\langle -|, \quad (\text{S4})$$

where  $r_+$  and  $r_-$  are the probabilities defined by  $r_- := r_{12} + r_{23} + r_{13}$ ,  $r_{ij} := p_i q_j + p_j q_i$ , and  $r_+ := 1 - r_-$  are probabilities, and  $\mathcal{C}_+$  and  $\mathcal{C}_-$  are the Pauli channels defined by

$$\mathcal{C}_+ = \frac{(\sum_{i=0}^3 r_{ii}/2)\rho + \sum_{i=1}^3 r_{0i} \sigma_i \rho \sigma_i}{\sum_i (r_{0i} + r_{ii}/2)} \quad (\text{S5})$$

and

$$\mathcal{C}_- = \frac{[r_{12} \sigma_3 \rho \sigma_3 + r_{23} \sigma_1 \rho \sigma_1 + r_{31} \sigma_2 \rho \sigma_2]}{r_{12} + r_{23} + r_{13}}. \quad (\text{S6})$$

If a bit flip channel ( $\mathcal{B}_s(\rho) = (1 - s)\rho + s\sigma_1\rho\sigma_1$ ) and a phase flip channel ( $\mathcal{P}_t(\rho) = (1 - t)\rho + t\sigma_3\rho\sigma_3$ ) are used, the output state is

$$\mathcal{S}(\mathcal{B}_s, \mathcal{P}_t)(\rho) = ((1 - t - s + 2ts)\rho + s(1 - t)\sigma_1\rho\sigma_1 + (1 - s)t\sigma_3\rho\sigma_3) \otimes |+\rangle\langle +|_c + (ts\sigma_2\rho\sigma_2) \otimes |-\rangle\langle -|_c, \quad (\text{S7})$$

$$r_- = s + t - 2ts, \quad r_+ = 1 - s - t + 2ts. \quad (\text{S8})$$

If two entanglement-breaking channels  $\mathcal{F}(\rho) = 1/2(\sigma_1\rho\sigma_1 + \sigma_2\rho\sigma_2)$  are used, the output state is

$$\mathcal{S}(\mathcal{F}, \mathcal{F})(\rho) = \rho/2 \otimes |+\rangle\langle +|_c + \sigma_3\rho\sigma_3/2 \otimes |-\rangle\langle -|_c, \quad (\text{S9})$$

$$r_- = \frac{1}{2}, \quad r_+ = \frac{1}{2}. \quad (\text{S10})$$

If two depolarizing channels  $\mathcal{D}(\rho) = 1/4 \sum_{i=0}^3 \sigma_i \rho \sigma_i$  are used, the output state is

$$\mathcal{S}(\mathcal{D}, \mathcal{D})(\rho) = (I/4 + \rho/8) \otimes |+\rangle\langle +|_c + (I/4 - \rho/8) \otimes |-\rangle\langle -|_c, \quad (\text{S11})$$

$$r_- = \frac{3}{8}, \quad r_+ = \frac{5}{8}. \quad (\text{S12})$$

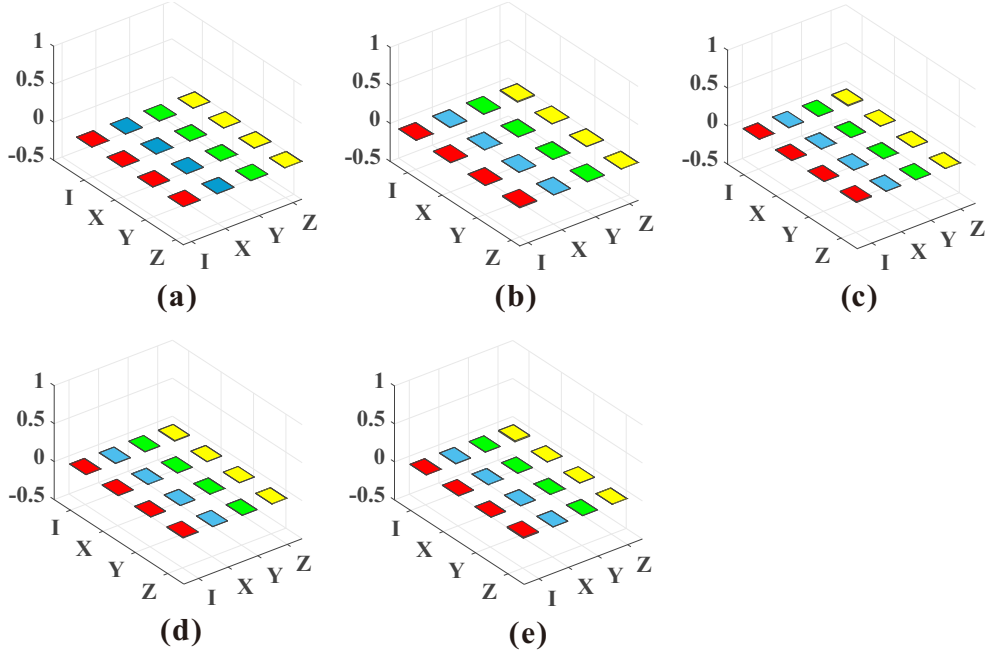


FIG. S2. The imaginary parts of the matrices of the channels: (a-b) for  $\mathcal{C}_+$  and  $\mathcal{C}_-$  of switched depolarizing channel  $\mathcal{S}(\mathcal{D}, \mathcal{D})$ , (c) for  $\mathcal{C}_-$  of switched dephasing channel  $\mathcal{S}(\mathcal{B}_s, \mathcal{P}_t)$  with  $s = t = 1/2$ , (d-e) for  $\mathcal{C}_+$  and  $\mathcal{C}_-$  of switched entanglement-breaking channel  $\mathcal{S}(\mathcal{F}, \mathcal{F})$ .

*Further information on the experimental results.*— Fig. S2 shows the imaginary parts of the matrices of the channels: Fig. S2(a-b) for  $\mathcal{C}_+$  and  $\mathcal{C}_-$  of switched depolarizing channel  $\mathcal{S}(\mathcal{D}, \mathcal{D})$ , Fig. S2(c) for  $\mathcal{C}_-$  of switched dephasing channel  $\mathcal{S}(\mathcal{B}_s, \mathcal{P}_t)$  with  $s = t = 1/2$ , Fig. S2(d-e) for  $\mathcal{C}_+$  and  $\mathcal{C}_-$  of switched entanglement-breaking channel  $\mathcal{S}(\mathcal{F}, \mathcal{F})$ .